

# Phase Separation and Liquid Crystal Self-Assembly in Surfactant–Inorganic–Solvent Systems

Flor R. Siperstein and Keith E. Gubbins\*

Department of Chemical Engineering, North Carolina State University,  
Raleigh, North Carolina 27695

Received August 15, 2002. In Final Form: November 23, 2002

The behavior of surfactant–inorganic oxide–solvent systems is studied using lattice Monte Carlo simulations. Under no inorganic condensation conditions, these systems phase separate into a liquid crystal phase that contains mainly surfactant and inorganic oxide, in equilibrium with a solvent-rich phase. In the systems studied, the solvent and the inorganic oxide have favorable interactions with the surfactant head, but the inorganic oxide–surfactant interactions are stronger than the solvent–surfactant interactions, which leads to a phase separation, regardless of the oxide–solvent miscibility. The formation of ordered liquid crystal phases is observed in the phase containing a high surfactant concentration, and the structure of this phase depends on the system composition and strength of the interactions. The formation of hexagonal and lamellar structures at different conditions is in qualitative agreement with experimental evidence on the formation of surfactant–silica liquid crystals and the synthesis of MCM-41 type materials. The effects of temperature and surfactant architecture are also investigated. We show that the increase in surfactant solubility in the solvent-rich phase with temperature can result in a lamellar to hexagonal transformation and that surfactants with small head/tail ratios favor the formation of lamellar phases.

## Introduction

Following the introduction of MCM-41 type materials,<sup>1</sup> the synthesis of surfactant-templated nanostructured materials has attracted the attention of the scientific community because it provides the possibility of tailoring pore size, geometry, and surface chemistry through control of the synthesis conditions. Potential applications of these materials range from separations and catalysis<sup>2</sup> to the production of biomimetic materials<sup>3</sup> and devices for optical and electronic applications.<sup>4</sup> Several synthesis protocols have been developed in the past 10 years and are the focus of recent reviews.<sup>5</sup> Different protocols involve a variety of surfactants (cationic, anionic, nonionic, and block copolymers) and a wide range of synthesis conditions including acid or alkaline synthesis and high or low surfactant concentration in the initial surfactant solution. The synthesis of ordered nanoporous materials has also been extended to several transition metal oxides, including TiO<sub>2</sub>, which can have applications in photocatalysis and sensors. Despite the extensive experimental effort to control the structure and composition of templated nanoporous materials, molecular modeling of the different processes has remained elusive, mainly due to the overlapping kinetic and thermodynamic effects.

Detailed molecular modeling of these syntheses is not yet possible, because current computers can accommodate neither the system size needed to have a representative sample of the material nor time scales sufficient to observe micelle formation. Simulations using detailed atomistic potentials have, for the most part, focused on the evolution of prearranged structures<sup>6</sup> but are usually unable to span real times that are long enough to observe formation and destruction of micelles.<sup>7,8</sup> Simulations containing all atom descriptions of prearranged structures of surfactant, solvent, and other ionic species are reported in the literature,<sup>9</sup> but as the authors point out, the structures relax during the course of the simulation and while they may reach an energy plateau they are not necessarily equilibrated systems. The obstacle for these systems to reach equilibrium and sample the whole phase space is that micelles have length scales that are much larger than those for individual amphiphiles. Due to this limitation, most of the work reported to study the formation of ordered materials is restricted to very simplified models on or off lattice.

Some coarse-grained simulations to study the formation of organic–inorganic ordered structures are reported in the literature.<sup>10–13</sup> Molecular simulations of two-dimensional ionic surfactants in the presence of neutral particles

\* To whom correspondence should be addressed. E-mail: keg@ncsu.edu.

(1) Beck, J. S.; Vartuli, J. C.; Roth, W. J.; Leonowicz, M. E.; Kresge, C. T.; Schmitt, K. D.; Chu, C. T.-W.; Olson, D. H.; Sheppard, E. W.; McCullen, S. B.; Higgins, J. B.; Schlenker, J. L. *J. Am. Chem. Soc.* **1992**, *114*, 10834.

(2) Tanev, P. T.; Chibwe, M.; Pinnavaia, T. J. *Nature* **1994**, *368*, 6469. Asefa, T.; MacLachan, M. J.; Coombs, N.; Ozin, G. A. *Nature* **1999**, *402*, 867.

(3) Davis, S. A.; Burkett, S. L.; Mendelson, N. H.; Mann, S. *Nature* **1997**, *385*, 420.

(4) Scott, B. J.; Wirnsberger, G.; Stucky, G. D. *Chem. Mater.* **2001**, *13*, 3140.

(5) Sayari, A.; Hamoudi, S. *Chem. Mater.* **2001**, *13*, 3151. Schüth, F. *Chem. Mater.* **2001**, *13*, 3184. Ciesla, U.; Schüth, F. *Microporous and Mesoporous Mater.* **1999**, *27*, 131. Ying, J. Y.; Mehnert, C. P.; Wong, M. S. *Angew. Chem., Int. Ed.* **1999**, *38*, 56.

(6) Bandyopadhyay, S.; Tarek, M.; Klein, M. L. *Curr. Opin. Colloid Interface Sci.* **1998**, *3*, 242.

(7) Shelley, J. C.; Shelley, M. Y. *Curr. Opin. Colloid Interface Sci.* **2000**, *5*, 101.

(8) Rajagopalan, R. *Curr. Opin. Colloid Interface Sci.* **2001**, *6*, 357.

(9) Mohanty, S.; Davis, H. T.; McCormick, A. V. *Langmuir* **2001**, *17*, 7160.

(10) Bhattacharya, A.; Mahanti, S. D. *J. Phys.: Condens. Matter* **2001**, *13*, 1413.

(11) Rankin, S. E.; Malanoski, A. P.; Van Swol, F. *Nonlithographic and Lithographic Methods of Nanofabrication: From Ultralarge-Scale Integration to Photonics to Molecular Electronics*; Materials Research Society Symposium Proceedings Vol. 636; Materials Research Society: Warrendale, PA, 2001; pp D1.2/1–D1.2/6.

(12) Lu, Y. F.; Ganguli, R.; Drewien, C. A.; Anderson, M. T.; Brinker, C. J.; Gong, W. L.; Guo, Y. X.; Soye, H.; Dunn, B.; Huang, M. H.; Zink, J. I. *Nature* **1997**, *389*, 364.

show that in order to have an ordered structure of the neutral particles around the micelles, the dimensionless density has to be sufficiently large that it corresponds to a liquid phase.<sup>10</sup> Other studies have involved lattice Monte Carlo simulation where the ordering of the surfactant liquid crystal phase is driven by evaporation of the solvent,<sup>11</sup> similar to what is observed in dip-coating techniques.<sup>12</sup> Computational studies of self-assembly of inorganic particles during spinodal decomposition have been reported.<sup>13</sup> In this paper, we are interested in describing the bulk synthesis of surfactant-templated silica materials, based on experimental evidence that surfactant-silica liquid crystal phases can be obtained under no silica polymerization conditions, where true lyotropic liquid crystal phases (hexagonal or lamellar) are in equilibrium with a solvent-rich phase that may contain a small amount of free surfactant and silica species.<sup>14</sup> These mesophases are prepared under highly alkaline conditions, from separate isotopic aqueous inorganic and surfactant precursors containing multiply charged anionic silicate oligomers and cationic micelles, respectively. In this work, we show that the formation of liquid crystal phases containing a high concentration of surfactant and inorganic oxide can be described by a simple lattice model. In this model, strong attraction between the surfactant and the inorganic oxide leads to the formation of liquid crystal phases despite the fact that many important factors, such as hydrogen bond type interactions, the presence of cosolvents, and the detailed composition of the solutions, are not considered.

Even when the existence of silica-surfactant lyotropic liquid crystal phases has been observed for cationic surfactants (cetyltrimethylammonium bromide, CTAB) under strongly basic conditions, in this work we model neutral surfactants under the assumption that this behavior is not specific to ionic surfactants but results from the absence of appreciable inorganic polymerization. On the other hand, synthesis methodologies using nonionic surfactants are especially interesting because the surfactant is only weakly bound to the silica framework and can be removed by solvent extraction without the need for calcination.

A wide variety of nonionic surfactants has been used for the synthesis of templated materials,<sup>15</sup> including alkyl-poly(ethylene oxide) oligomeric surfactants ( $C_nEO_m$ )<sup>16</sup> and triblock copolymers of the Pluronic family.<sup>17</sup> In general, for a given alkyl chain length, lamellar structures were observed for short ethylene oxide (EO) chains, while the formation of cubic and hexagonal phases was favored with long EO chains. However, surfactants with long EO chains ( $C_{12}EO_{23}$  or  $C_{16}EO_{20}$ ) did not promote the silica precipitation. For a given surfactant, such as  $C_{16}EO_{10}$ , cubic structures (SBA-11) were formed from solutions containing low surfactant/silica ratios and lamellar structures were formed at high surfactant/silica ratios. The type of structures obtained from several nonionic alkyl-ethylene oxide surfactants at different surfactant/silica concentrations are summarized in Table 1.

Given the complexity of the synthesis of surfactant-templated silica materials and the many variables that

**Table 1. Synthesis Conditions for Different Mesoporous Silica Structures<sup>a</sup>**

surfactant	surfactant/silica <sup>b</sup>	structure
$C_{12}EO_4$	<0.2	cubic
	>0.3	lamellar
$C_{12}EO_{23}$	<0.042	cubic
	>0.042	no precipitation or gel formation
$C_{16}EO_2$		lamellar
$C_{16}EO_{10}$	<0.036	partial precipitation
	0.036–0.6	cubic
	>0.6	lamellar
$C_{16}EO_{20}$	<0.047	cubic
	>0.047	no precipitation or gel formation
		three-dimensional
$C_{18}EO_{10}$	0.03–0.5	hexagonal
CTAB(20% NaOH)	0.025–0.14	hexagonal
	0.33–1.0	cubic
	1.0–1.67	lamellar

<sup>a</sup> Reference 16. <sup>b</sup> Mole ratio.

can have an influence on the structure and properties of the final product, it would be impossible to include all of them in this study. Thus, we do not attempt to investigate all the variables involved in the synthesis of surfactant-templated silica materials but rather select the governing factors that can be used to describe the physics of these syntheses. For the problem of interest in this work, it is necessary to study a system that is large enough so that the mesoscopic periodicity can be observed, while retaining a simplified description of the surfactant. Therefore, we selected lattice simulations because they allow large systems to be studied.

We study the equilibrium properties of ordered mesoporous silica materials, with linear nonionic diblock surfactants as structure-directing agents. The key to predicting structures of templated mesoporous materials is to understand how a dilute solution with spherical micelles becomes a liquid crystal phase when silica is added to the system. We show that synthesis of templated materials in bulk solution can be interpreted with an equilibrium triangular diagram for surfactant, solvent, and silica, where different liquid crystal phases can be located. The equilibrium diagram is calculated using a lattice Monte Carlo approach, specifying the appropriate interaction parameters to represent each component. The phase behavior is studied as a function of silica/water solubility, temperature, and surfactant compositions. A favorable interaction between the silica and the surfactant head produces an immiscibility gap inside the ternary diagram; the shape and location of the immiscibility gap determine the different liquid crystal phases that can be formed. In this work, we do not distinguish between different soluble silica species that may be present in real systems, such as monomers, dimers, and cyclic oligomers (double three rings and double four rings),<sup>14</sup> but we use an effective silica species that has favorable attractive interactions with the surfactant head.

### Simulation Method

Lattice Monte Carlo simulations have been used for over a decade to study micellization processes and to determine binary and ternary phase diagrams containing spherical micelles and hexagonal, lamellar, and cubic structures. Generally, the model surfactant molecules are made up of  $m$  hydrophilic headgroups H and  $n$  hydrophobic tailgroups T, that is,  $H_mT_n$ , and are distributed across lattice sites with one group per site. A site on the surfactant chain can be connected to any of its  $z = 26$  nearest

(13) Balazs, A. C.; Ginzburg, V. V.; Qiu, F.; Peng, G. W.; Jasnow, D. *J. Phys. Chem. B* **2000**, *104*, 3411. Thompson, R. B.; Ginzburg, V. V.; Matsen, M. W.; Balazs, A. C. *Science* **2001**, *292*, 2469.

(14) Firouzi, A.; Atef, F.; Oertli, A. G.; Stucky, G. D.; Chmelka, B. *J. Am. Chem. Soc.* **1997**, *119*, 3596.

(15) Tanev, P. T.; Pinnavaia, T. J. *Science* **1995**, *267*, 865.

(16) Zhao, D.; Huo, Q.; Feng, J.; Chmelka, B. F.; Stucky, G. D. *J. Am. Chem. Soc.* **1998**, *120*, 6024.

(17) Zhao, D.; Feng, J.; Huo, Q.; Melosh, N.; Fredrickson, G. H.; Chmelka, B. F.; Stucky, G. D. *Science* **1998**, *279*, 548.

neighbors or diagonally nearest neighbors. Solvent molecules, S, occupy single sites, and oil molecules if present occupy one or several sites.<sup>18–25</sup>

In this work, the simulations in the canonical ensemble were performed on a three-dimensional lattice, following the model presented by Larson et al.<sup>18</sup> Following our previous work,<sup>26</sup> each segment of the surfactant (H<sub>4</sub>T<sub>4</sub>, H<sub>4</sub>T<sub>6</sub>, or H<sub>2</sub>T<sub>6</sub>), solvent, or inorganic can occupy a single point on the lattice. The solvent (S) and the inorganic component (I) occupy a single site on the lattice, while the surfactant occupies several connected sites.

Each molecular unit (H, T, S, and I) is characterized by an interaction energy  $\epsilon_{ij}$  ( $i, j = \text{H, T, S, I}$ ). The total energy of the system is given by

$$E = \frac{1}{2} \sum_i \sum_j N_{ij} \epsilon_{ij} = \sum_i N_{ii} \epsilon_{ii} + \frac{1}{2} \sum_i \sum_{j \neq i} N_{ij} \epsilon_{ij} \quad (1)$$

where  $N_{ij}$  are the number of contacts between species of kind  $i$  and  $j$ . For a lattice with coordination number  $z$  and  $n_i$  molecules of type  $i$ , a balance over the number of contacts can be expressed as

$$zn_i = 2N_{ii} + \sum_{j \neq i} N_{ij} \quad (2)$$

Substitution of eq 2 into eq 1 gives

$$E = \frac{1}{2} \sum_i (zn_i - \sum_{j \neq i} N_{ij}) \epsilon_{ii} + \frac{1}{2} \sum_i \sum_{j \neq i} N_{ij} \epsilon_{ij} = \frac{1}{2} \sum_i zn_i \epsilon_{ii} + \frac{1}{2} \sum_i \sum_{j \neq i} N_{ij} (\epsilon_{ij} - \epsilon_{ii}) \quad (3)$$

In a canonical ensemble, the difference in energy between two configurations is given by

$$\Delta E = \frac{1}{2} \sum_i \sum_{j \neq i} (\epsilon_{ij} - \epsilon_{ji}) \Delta N_{ij} \quad (4)$$

Notice that  $N_{ij} = N_{ji}$  and  $\epsilon_{ij} = \epsilon_{ji}$ . Therefore, the net energy change associated with any configurational rearrangement depends on a set of interchange energies  $\omega_{ij}$ ,

$$\omega_{ij} = \frac{1}{2} (\epsilon_{ij} + \epsilon_{ji} - \epsilon_{ii} - \epsilon_{jj}) = \epsilon_{ij} - \frac{1}{2} (\epsilon_{ii} + \epsilon_{jj}) \quad \text{with } i \neq j \quad (5)$$

and not on the individual interaction energies  $\epsilon_{ij}$ . The dimensionless temperature is defined using the head–tail interchange energy by  $T^* = k_B T / \omega_{HT}$ . The surfactant–solvent interaction parameters are the same as those used by other researchers:<sup>22–24</sup>  $\omega_{HT} = \omega_{ST}$  and  $\omega_{HS} = 0$ . A strong inorganic–head attraction to mimic the strong affinity between silica and surfactant heads was specified as  $\omega_{IH} = -2\omega_{HT}$ , and  $\omega_{IT} = \omega_{HT}$  or  $\omega_{IT} = 0$ . Two extreme cases

**Table 2. Individual Interaction Parameters ( $\epsilon_{ij}$ )**

	H	T	S	I
1. complete miscibility between inorganic oxide and solvent <sup>a</sup>				
H	0	0	0	-2
T	0	-2	0	0
S	0	0	0	0
I	-2	0	0	0
2. inorganic oxide and solvent partially immiscible <sup>b</sup>				
H	0	0	0	-3
T	0	-2	0	-2
S	0	0	0	0
I	-3	-2	0	-2

<sup>a</sup>  $\omega_{HT} = 1$ ,  $\omega_{HS} = 0$ ,  $\omega_{TS} = 1$ ,  $\omega_{HI} = -2$ ,  $\omega_{TI} = 1$ ,  $\omega_{SI} = 0$ .  
<sup>b</sup>  $\omega_{HT} = 1$ ,  $\omega_{HS} = 0$ ,  $\omega_{TS} = 1$ ,  $\omega_{HI} = -2$ ,  $\omega_{TI} = 0$ ,  $\omega_{SI} = 1$ .

were studied, one where the inorganic component and the solvent are completely miscible ( $\omega_{IS} = 0$ ) and another where they are immiscible ( $\omega_{IS} = \omega_{HT}$ ). Experimentally, the solubility of tetraethoxysilane (TEOS) in water depends on the alcohol content of the mixture.<sup>27</sup> In a strict sense, the solubility of TEOS changes as the condensation takes place, since alcohol is produced during the reaction. In this work, the solubility of the inorganic oxide does not change during the simulation, since we work under the assumption that condensation is negligible at these conditions.

The parameters  $\epsilon_{SJ}$  (where  $J = \text{H, T, S, or I}$ ) were set to zero, and the rest of the individual interactions were rescaled to obtain the appropriate values of  $\omega_{S,J}$ . The individual values of  $\epsilon_{ij}$  relative to  $\omega_{HT} = 1$  are summarized in Table 2.

All Monte Carlo simulations were performed in the canonical ensemble (NVT) with periodic boundary conditions. Reptation and “kink”-like moves were considered in addition to chain regrowth using the configurational bias method.<sup>28</sup> Cluster moves were implemented to sample the phase space more efficiently. Surfactants are considered to be part of a cluster (or micelle) if they have at least one tail segment in contact with another surfactant in the cluster. Cluster moves were restricted to clusters containing less than 200 chains and were 1000 times less frequent than other types of moves.

Properties of binary systems (surfactant–solvent or surfactant–inorganic oxide) were calculated for cubic boxes in the canonical ensemble using periodic boundary conditions. The box sizes were varied between  $20^3$  and  $80^3$  to ensure that the structures obtained were independent of the box size. As was reported by Larson,<sup>22</sup> hexagonally ordered cylindrical micelles and lamellar phases can be obtained regardless of the size of the box, as long as the simulation box is larger than one unit cell. Cubic structures cannot be obtained unless the box size matches the periodicity of the system.

Ternary liquid–liquid equilibria were calculated using a direct interfacial approach. One dimension of the simulation box was increased with respect to the other two by a factor of 8 to favor the formation of two pseudo-flat interfaces.<sup>23</sup> The box size used in the simulation was  $40 \times 40 \times 320$  sites, and periodic boundary conditions were used in all directions. This simulation box is large enough to observe at least three times the periodicity of the surfactant liquid crystal, which can be considered large enough not to have an important influence from the box size.

(27) Wright, J. D.; Sommerdijk, N. A. J. M. *Sol–Gel Materials, Chemistry and Applications*; Gordon and Breach Science: Amsterdam, 2001; pp 17–18.

(28) Frenkel, D.; Smit, B. *Understanding Molecular Simulation*; Academic Press: San Diego, 1996.

(18) Larson, R. G.; Scriven, L. E.; Davis, H. T. *J. Chem. Phys.* **1985**, *83*, 2411.

(19) Larson, R. G. *J. Chem. Phys.* **1989**, *91*, 2479.

(20) Larson, R. G. *J. Chem. Phys.* **1992**, *96*, 7904.

(21) Talsania, S. K.; Wang, Y.; Rajagopalan, R.; Mohanty, K. K. *J. Colloid Interface Sci.* **1997**, *190*, 92.

(22) Larson, R. G. *J. Phys. II France* **1996**, *6*, 1441.

(23) Mackie, A. D.; Onur, K.; Panagiotopoulos, A. Z. *J. Chem. Phys.* **1996**, *104*, 3718.

(24) Mackie, A. D.; Panagiotopoulos, A. Z.; Szleifer, I. *Langmuir* **1997**, *13*, 5022.

(25) Floriano, M. A.; Onur, K.; Panagiotopoulos, A. Z. *Langmuir* **1999**, *15*, 3143.

(26) Siperstein, F. R.; Gubbins, K. E. *Mol. Simul.* **2001**, *27*, 339.

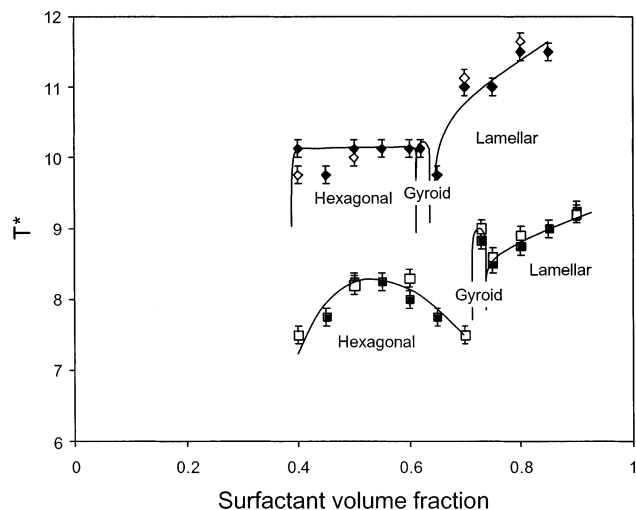


**Figure 1.** Surfactant/water phase diagram for  $H_4T_6$  ( $\blacklozenge$ ,  $\diamond$ ) and  $H_4T_4$  ( $\blacksquare$ ,  $\square$ ). The solid symbols are from ref 22, and the open symbols are our results.

Bulk coexisting densities were estimated from ensemble averages of the system densities away from the interfaces after the system reached equilibrium. The reduced temperature was chosen to be the same as that used by Larson in his work ( $T^* = 6.5$ ). Up to 125 000 cycles were needed for the system to equilibrate, where each cycle consists of  $40 \times 40 \times 320$  configurations.

The starting configuration was obtained as follows. A box containing a high surfactant concentration, 60 vol % of surfactant, was equilibrated at infinite temperature on a  $40 \times 40 \times 40$  or  $40 \times 40 \times 80$  lattice with periodic boundary conditions in the  $x$  and  $y$  directions and hard walls in the  $z$  direction. After equilibration, the box with the high surfactant concentration was placed in the  $40 \times 40 \times 320$  box, resulting in a slab having 60% surfactant. Inorganic oxide units and solvent units were distributed randomly over the whole  $40 \times 40 \times 320$  box, not allowing for overlaps with the previously arranged surfactant chains. This selection of initial configuration favored the formation of only two interfaces. The overall surfactant concentration of such a box varied between 6.5 and 15% in volume.

Different density profiles were used as the initial configuration for the ternary liquid–liquid equilibrium calculations as a check that the results obtained were not an artifact of the initial configuration of the system. Some simulations were carried out starting from a completely homogeneous box containing free surfactants, silica, and solvent randomly distributed, and others starting from a box containing homogeneously distributed spherical micelles, solvent, and silica. The equilibration time was considerably longer than in the case where a high surfactant concentration slab was used as the initial configuration, and the formation of more than two interfaces was observed in some cases. Nevertheless, the compositions far from the interface were independent of the initial configuration.

## Results and Discussion

**Binary Mixtures.** The phase behavior of the surfactant ( $H_4T_4$  and  $H_4T_6$ )–solvent systems, with the interaction parameters we used, has been reported in the literature.<sup>22,29</sup> Figure 1 shows the binary phase diagrams for these two surfactants studied in water, indicating good

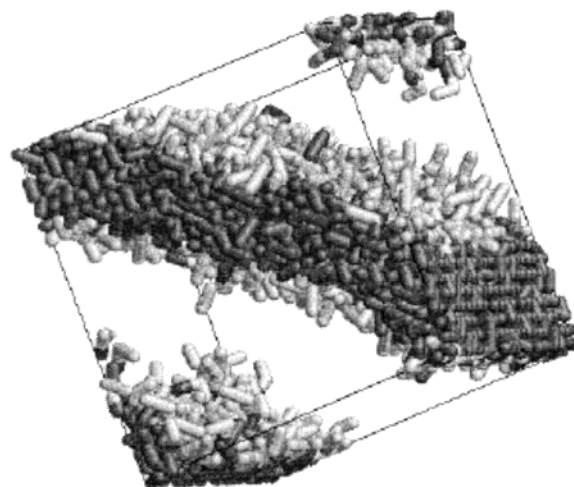


**Figure 2.** Bilayer structure observed for  $H_2T_6$  at  $T^* = 9$  and surfactant volume fractions of 40% for a  $24^3$  simulation box. Surfactant heads are shown in light gray, and surfactant tails in dark gray.

agreement with previously reported results. Since gyroid phases tend to appear in such a narrow range of concentrations and the order–disorder transition is much more sensitive to the box dimensions than these involving hexagonal or lamellar phases,<sup>22</sup> we made no attempt to pinpoint the concentration, or box dimensions, where this phase can be observed. The order–disorder transition temperature is the highest temperature at which the surfactant forms ordered structures.

Surfactants with a small head/tail ratio are not completely miscible with water, and phase separation is observed at small enough concentrations such that micellization is prevented.<sup>29,30</sup> Nevertheless, in some cases, the formation of ordered structures at high surfactant concentration can be observed. The third surfactant studied ( $H_2T_6$ ) does not form micelles at low surfactant concentrations, but at surfactant concentrations above 40% and  $T^* < 9.5$  it is possible to observe the formation of a bilayer and at higher concentrations lamellar arrangements (Figure 2).

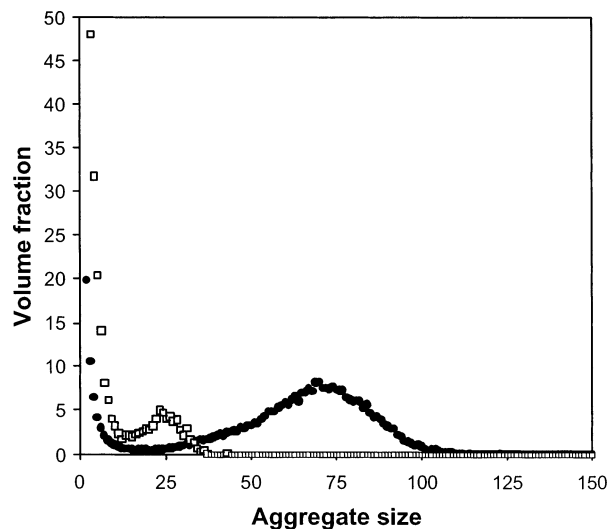
Even when lattice simulations of surfactants are used over a wide range of conditions, it is important to keep in mind that the model used does not reproduce all the features of surfactant/water systems, such as the presence of a lower critical solution temperature (LCST) observed in nonionic surfactant solutions.<sup>31</sup> If we restrict ourselves to studying the behavior of surfactants in a narrow range of temperatures, far below the LCST, lattice simulations can provide important insight into the physics of these systems. When working near the LCST region, it is necessary to include in the description of the model the directional interaction of the hydrogen bonds to have a good representation of the system studied.

Figure 3 shows the aggregate size distribution for  $H_4T_4$ /water and  $H_4T_4$ /inorganic at  $T^* = 6$  for a surfactant volume fraction of 0.05. The aggregate size distribution is independent of the size of the system as can be seen in Figure 4, where the aggregate size distribution of  $H_4T_4$ /water is calculated in a  $40^3$  and  $80^3$  simulation box at the same volume fraction. The micelle size distribution was obtained by averaging during the simulation following system

(30) Kumar, S. K.; Floriano, M. A.; Panagiotopoulos, A. Z. *Adv. Chem. Eng.* **2001**, *28*, 297.

(31) Kuniieda, H.; Kabir, H.; Aramaki, K.; Shigeta, K. *J. Mol. Liq.* **2001**, *90*, 157–166. Strey, R. *Ber. Bunsen-Ges. Phys. Chem.* **1996**, *100*, 182.

(29) Panagiotopoulos, A. Z.; Floriano, M. A.; Kumar, S. K. *Langmuir* **2002**, *18*, 2940.



**Figure 3.** Micelle size distribution for  $H_4T_4$ /water (■) and  $H_4T_4$ /silica (□) at  $T^* = 6$  using the first set of interaction parameters (Table 2.1) for the surfactant–silica interactions.

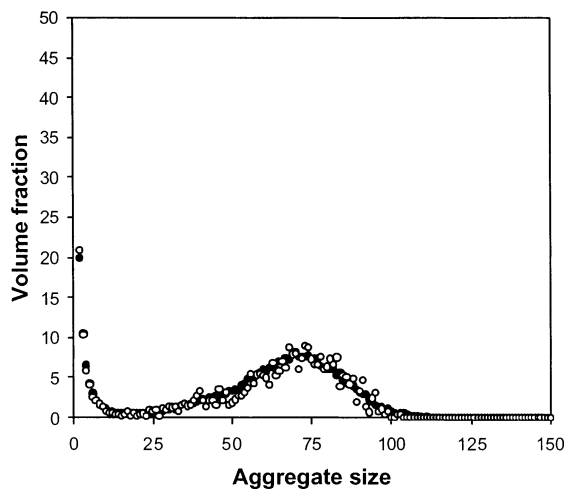


**Figure 4.** Micelle size distribution for  $H_4T_4$ /water at  $T^* = 6$  for a simulation box of  $40^3$  (○) and  $80^3$  (●).

equilibration, following standard procedures.<sup>25</sup> Micelles of  $H_4T_4$  in water at this temperature have an average size of 70 surfactant chains, while the  $H_4T_4$ /inorganic mixture has an average micelle size of only 24 due to the more favorable interactions between the surfactant head and the inorganic component ( $\omega_{HI} = -2$ ) compared to the water/surfactant head interactions ( $\omega_{HS} = 0$ ). Even when the areas under both curves in Figure 3 are the same, the fraction of free surfactants and aggregates of up to 5 surfactant chains in  $H_4T_4$ /water is less than 25% of the total surfactant concentration while for  $H_4T_4$ /inorganic these small aggregates constitute approximately 75% of the total surfactants. Nevertheless, there is a clear aggregate size that is more favorable in each case, indicating the formation of micelles.

Figure 5 contains the binary phase diagram for the  $H_4T_4$ /inorganic binary system. Cylindrical micelles ordered in a hexagonal arrangement are observed in the same range of concentrations as the  $H_4T_4$ /water systems, but due to the different interaction parameters, hexagonal and lamellar phases in the  $H_4T_4$ /inorganic binary system are stable in a wider temperature range than in the  $H_4T_4$ /water system. The formation of perforated lamellae was observed at high surfactant concentration. It is likely that cubic or gyroid phases would also be observed at these

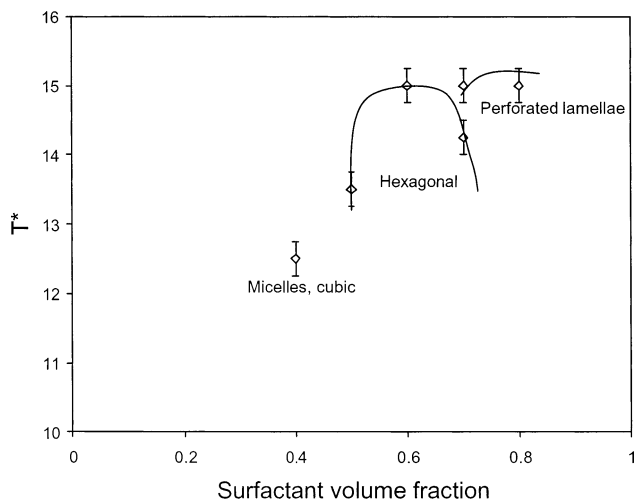


**Figure 5.**  $H_4T_4$ /silica phase diagram using the first set of interaction parameters in Table 2 for the surfactant–silica interactions.

concentrations if the box dimensions were chosen appropriately.<sup>22</sup> At low surfactant concentrations, spherical micelles are observed, as in the  $H_4T_4$ /water system, but in this case the micelles are considerably smaller due to the favorable interactions between the surfactant head and the silica.

**Ternary Mixtures.** Typical density profiles observed during the simulations for ternary mixtures are shown in Figure 6. The formation of spherical micelles was observed at small silica concentrations, where no phase separation was observed. In the cases where phase separation was observed, the final surfactant concentration in the high surfactant concentration slab varied between 40 and 90%. During the equilibration period, the center of the high surfactant concentration slab moved along the  $z$ -axis of the simulation box, but once the system was equilibrated, there was no significant displacement of the ordered liquid crystal phase. Some examples of the structure of the inorganic component after the system is equilibrated are shown in Figure 7.

In Figure 8 and Figure 9, we show ternary phase diagrams for water/surfactant/inorganic oxide systems that were calculated at a dimensionless temperature  $T^* = 6.5$  with the interaction parameters in Table 2. This temperature is approximately 15% lower than that of the order–disorder transition temperature, ensuring that the system is held at conditions significantly below the LCST observed in nonionic surfactants such as  $C_{12}EO_6$ .<sup>32</sup> The main difference between Figure 8 and Figure 9 is the water/inorganic oxide solubility. In Figure 8,  $\omega_{SI} = 0$  and water and silica are completely miscible, while in Figure 9  $\omega_{SI} = \omega_{HT}$  and the silica/water solubility is 2.5 vol %. The difference in solubilities is a result of the interaction parameters defined in eq 5. In both cases, phase separation and coexistence of a surfactant–silica liquid crystal phase in equilibrium with a solvent-rich phase are observed. The driving force for the phase separation is the strong silica–surfactant head interactions.

Phase separation in a ternary system where two of the possible binary mixtures are completely miscible can be achieved either by an effective attraction between two components strong enough to form a two-phase region or by an effective repulsion between molecules of two different components that is sufficiently strong to induce the phase

(32) Mitchell, J.; Tiddy, G. J. T.; Waring, L.; Bostock, T.; McDonald, M. P. *J. Chem. Soc., Faraday Trans. 1* **1983**, *79*, 975.

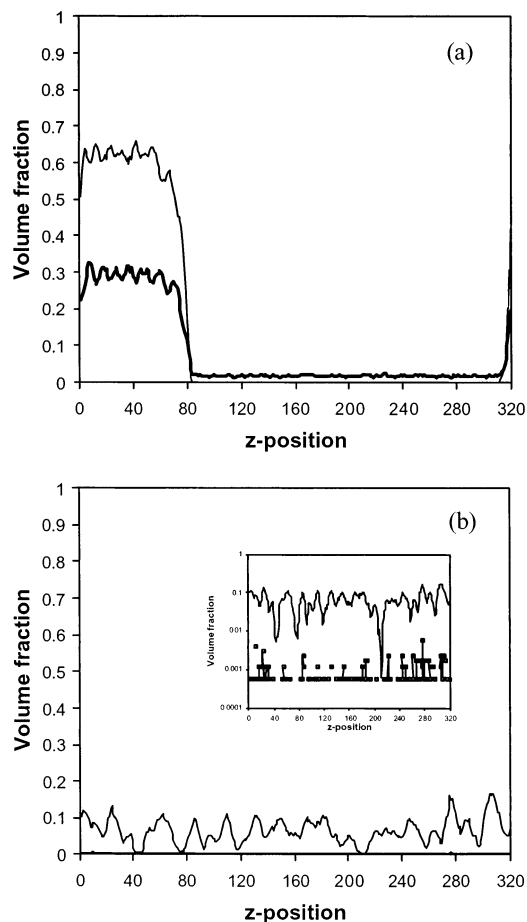


**Figure 6.** Typical composition profile of a single snapshot for a ternary mixture (parameters given in Table 2.1) in a  $40 \times 40 \times 320$  simulation box at  $T^* = 6.5$  along the  $z$  direction. The thick line corresponds to the silica volume fraction, and the thin line to the surfactant ( $H_4T_4$ ) volume fraction. (a) A system with phase separation; the overall composition (by volume) is 15% surfactant and 8.5% inorganic oxide. (b) A system with no phase separation but with formation of micelles, with an overall composition (by volume) of 6.5% surfactant and 0.04% inorganic oxide.

separation. The former process is known as associative and the latter as segregative phase separation.<sup>33</sup> Associative phase separation has been observed in systems containing a polyelectrolyte (hyaluronate) and a cationic surfactant (alkyltrimethylammonium bromide).<sup>34</sup>

The associative phase diagram in Figure 8 is similar to the behavior observed for the ternary system water–sodium hyaluronate (NaHy)–alkyltrimethylammonium bromide (CTAB) in the absence of salt<sup>34</sup> where the NaHy–CTAB interactions are stronger than the water–CTAB interactions. The similarity between the simulation results of a model surfactant–water–silica system and CTAB–water–NaHy is expected, since at the synthesis conditions the silica source is a highly charged oligomer, and silica–surfactant interactions are stronger than surfactant–water interactions. An important difference between the surfactant–solvent–silica and CTAB–water–NaHy systems reported by Thalberg et al.<sup>34</sup> is that for the latter the high surfactant concentration phase contains no more than 30% of surfactant, which probably is not enough to observe the formation of surfactant liquid crystal phases.

(33) Picullel L.; Lindman, B. *Adv. Colloid Interface Sci.* **1992**, *41*, 149.

(34) Thalberg, K.; Lindman, B.; Karlström, G. *J. Phys. Chem.* **1990**, *94*, 4289.

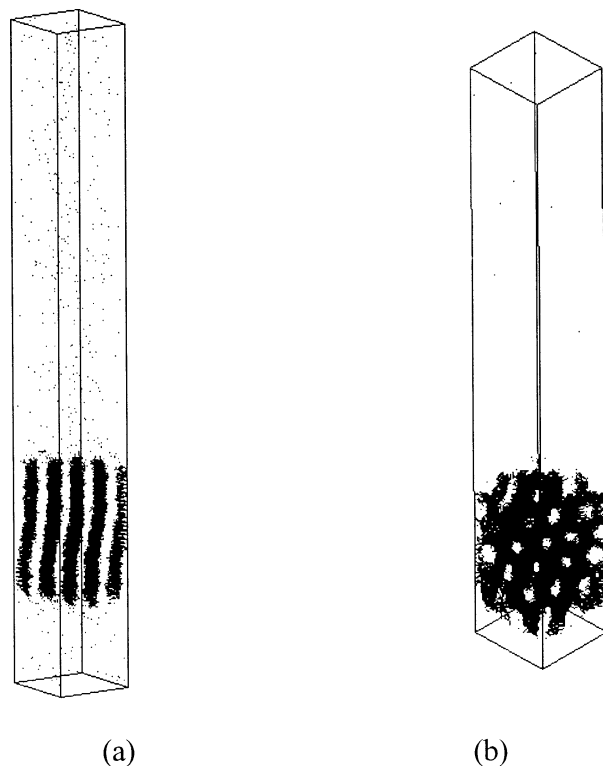


**Figure 7.** Silica structures formed at  $T^* = 6.5$  (a) for a miscible silica/water system with surfactant/silica = 1.0 and (b) for an immiscible silica/water system with surfactant/silica = 0.5. Surfactants were removed for visualization.

Also shown in Figure 8 and Figure 9 are the regions where hexagonal and lamellar phases are observed. In both cases, independent of the silica/water solubility, hexagonal phases are observed at high silica/surfactant ratios whereas lamellar phases are observed at lower silica/surfactant ratios, similar to what is known for the synthesis of MCM-41.<sup>35</sup> To compare our simulation results to experimental measurements of silica–surfactant liquid crystals,<sup>36</sup> it is necessary to assume that all simulations were carried out at a constant content of NaOH since we are not including the ions in solution explicitly but just taking effective interactions. It can be assumed that the simulations presented here correspond to a CTAB/water/silica system with a NaOH content of 20%,<sup>36</sup> where hexagonal phases are observed for surfactant/silica ratios between 0.025 and 0.14 and lamellar phases appear for surfactant/silica ratios between 1 and 1.67 (see Table 1). In our simulations, we observe hexagonal phases for surfactant/silica ratios between 0.16 and 0.5 and lamellar phases for surfactant/silica ratios larger than 1.0. It is clear that we are able to capture the qualitative trend in the structure observed as a function of the surfactant/silica ratio but are not able to obtain quantitative agreement. This is to be expected, since the surfactant used as a model does not closely resemble CTAB and, more importantly, the lattice coordination number determines the maximum number of surfactants that can interact with a silica unit. The difference in coordination number between the real materials and those specified in the simulation can account for the numerical discrepancy.

(35) Vartuli, J. C.; Schmitt, K. D.; Kresge, C. T.; Roth, W. J.; Leonowicz, M. E.; McCullen, S. B.; Hellring, S. D.; Beck, J. S.; Schlenker, J. L.; Olson, D. H.; Sheppard, E. W. *Chem. Mater.* **1994**, *6*, 2317.

(36) Firouzi, A.; Kumar, K.; Bull, L. M.; Besier, T.; Sieger, P.; Huo, Q.; Walker, S. A.; Zasadzinski, J. A.; Glinka, C.; Nicol, J.; Margolese, D.; Stucky, G. D.; Chmelka, B. F. *Science* **1995**, *267*, 1138.

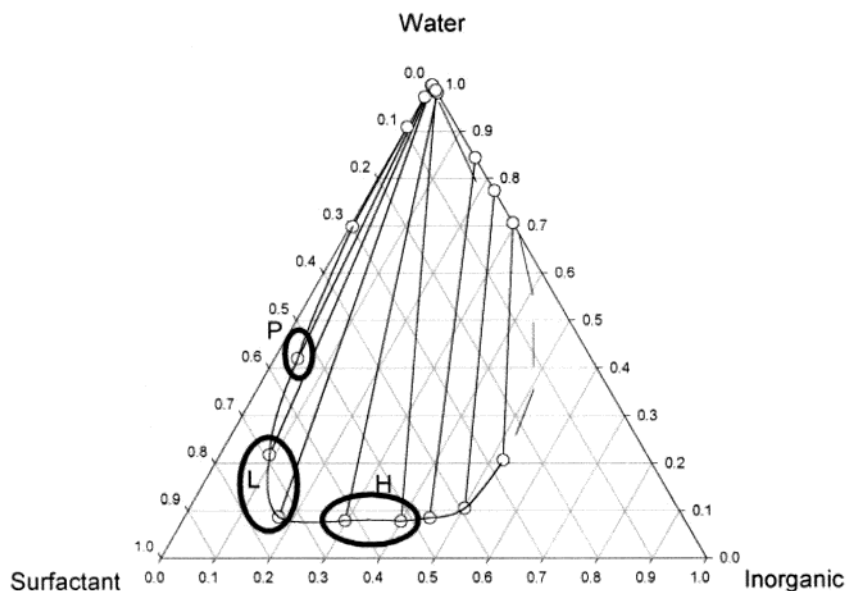


**Figure 8.** Associative ternary diagram  $H_4T_4$ /water/silica at  $T^* = 6.5$ , with parameters from Table 2.1. Circles indicate regions where hexagonal (H), lamellar (L), and perforated lamella (P) are observed.

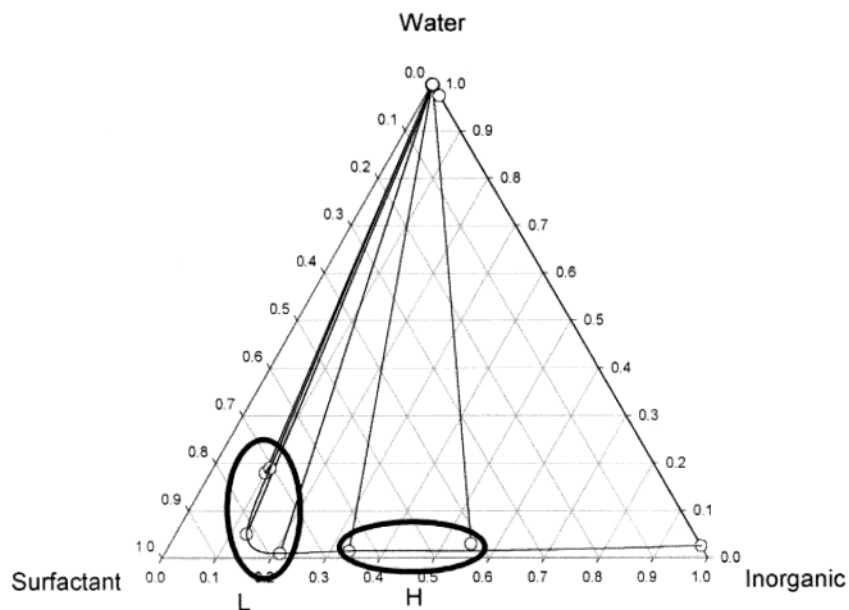


**Figure 9.** Segregative ternary diagram  $H_4T_4$ /water/silica at  $T^* = 6.5$ , with parameters from Table 2.2. Circles indicate regions where hexagonal (H) and lamellar (L) phases are observed.

Nevertheless, the qualitative agreement is remarkable considering the simplicity of the model.

It is important to notice that we do not observe the formation of a hexagonal phase for very low silica concentration. Even at a surfactant concentration of 55 vol %, where cylindrical micelles arranged in an hexagonal structure would be expected, a small amount of silica (5%) is enough to transform the hexagonal structure into a perforated lamellar structure (see Figure 8, point marked as P). Although the perforated lamellar structure is not found experimentally, it is interesting to notice that on increasing the surfactant concentration in CTAB/silica/water systems containing 20% of NaOH it is not possible to obtain any structure after the lamellar structure; for higher NaOH content, however, it is possible to have hexagonal structures at surfactant/silica ratios higher and lower than those needed for lamellar structures. In our model, the formation of a surfactant/silica liquid crystal is observed only when the silica–surfactant head attrac-

tion is stronger than that for the solvent–surfactant head. For the case of the associative phase separation, the system is completely miscible for equivalent interactions between the silica–surfactant head and solvent–surfactant head; this is similar to the behavior of surfactant–silica liquid crystals at high NaOH content. For the segregative phase separation case, when the silica–surfactant and solvent–surfactant interactions are equivalent, the surfactant is partitioned in both phases without the formation of liquid crystals. A direct relationship with experiments is complicated since the type of silicate species in solution, as well as the thickness of the Debye layers, depends on the NaOH content. From our simulations, it is possible to conclude that an increase in NaOH content can be represented effectively as a decrease in the surfactant–silica interaction strength.

No cubic phases were found, although they are observed experimentally at a surfactant/silica ratio of 1.0. The formation of cubic phases requires precise dimensions of

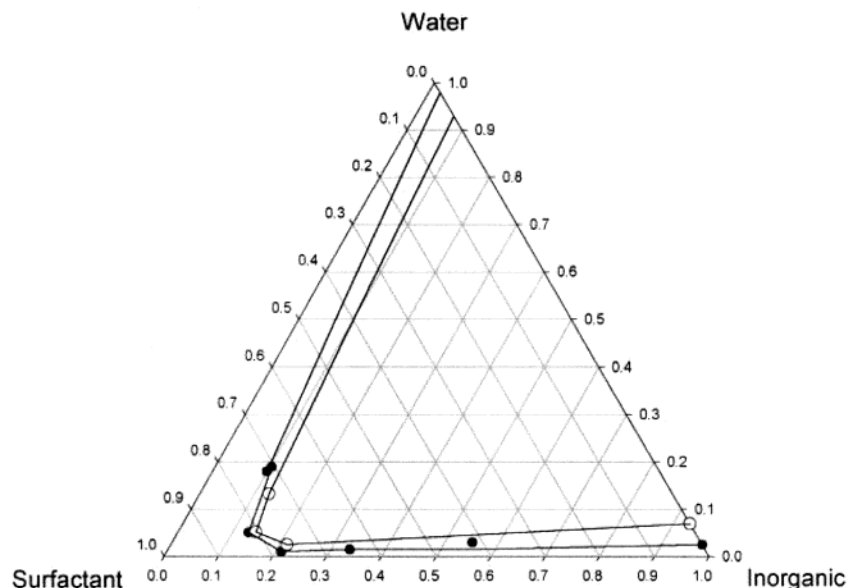


**Figure 10.** Segregative ternary diagram  $H_4T_4$ /water/silica at  $T^* = 6.5$  (●) and  $T^* = 7.5$  (○), with parameters from Table 2.2.

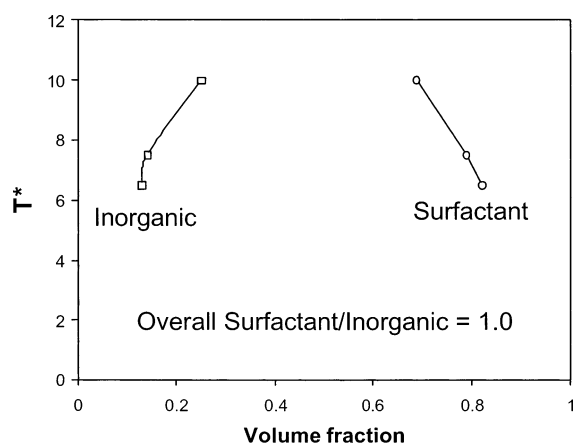


**Figure 11.** Temperature dependence of the composition of the liquid crystal phase for an overall  $H_4T_4$ /silica ratio of 1.0 for the case where the inorganic component and the solvent are immiscible: surfactant (○); inorganic (□).

the simulation box<sup>20</sup> but is expected in the region between lamellar and hexagonal phases.

**Temperature Dependence.** A comparison of segregative phase diagrams (when the inorganic oxide is partially immiscible with water) at different temperatures is shown in Figure 10. In this figure, solid symbols correspond to  $T^* = 6.5$  while open symbols correspond to  $T^* = 7.5$ . It is clear that as temperature increases, the two-phase immiscibility region becomes smaller, but the orientation of the tie lines in the diagram does not change significantly. For a given overall system composition, increasing the temperature results in a lower surfactant concentration in the surfactant-rich phase, but also in a higher silica concentration for the case where silica and solvent are not miscible. The decrease in the surfactant concentration with temperature in the surfactant-rich phase favors the formation of hexagonal phases at high temperatures and lamellar phases at low temperatures (Figure 11). This behavior is similar to that observed experimentally for the transformations of lamellar to hexagonal phases for CTAB–silica–water systems<sup>14</sup> where reversible lamellar to hexagonal transformations were observed when heating the system from 25 to 60 °C. The behavior is also similar to that of some nonequilibrium

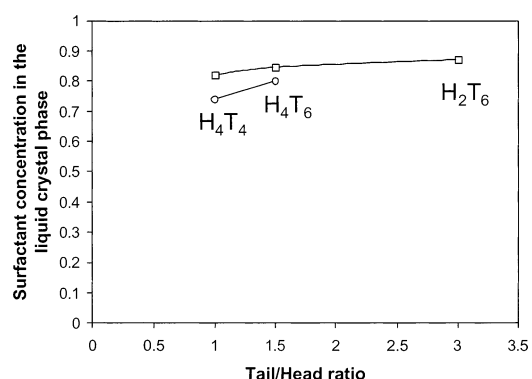


**Figure 12.** Surfactant volume fraction in the liquid crystal phase for different surfactants at  $T^* = 6.5$ . Squares are for the case when the inorganic component is partially immiscible in the solvent (parameters of Table 2.2), and circles are when the inorganic and solvent are completely miscible (parameters of Table 2.1).

systems that contain trimethylbenzene as a cosurfactant,<sup>37</sup> where the trimethylbenzene solubility in water increases with temperature, giving the same effect as we observe in the simulations, where our model surfactant solubility increases with temperature. As mentioned before, to observe the decrease in surfactant solubility with temperature it is necessary to include directional interactions in the surfactant–solvent description.

**Surfactant Composition.** Three surfactants ( $H_4T_4$ ,  $H_4T_6$ , and  $H_2T_6$ ) were studied at a surfactant/inorganic ratio of 1.0 and  $T^* = 6.5$ . Figure 12 shows that the surfactant concentration in the surfactant liquid crystal phase increases with decreasing head/tail ratio independently of the solubility of the inorganic in the solvent. Therefore, for a given overall system composition, surfactants with a small head/tail ratio will form lamellar phases and those with a large head/tail ratio will form hexagonal phases, in agreement with experimental observations.<sup>16</sup>

### Conclusions

We have shown that a simple lattice model can capture much of the physics behind the synthesis of surfactant-

(37) Tolbert, S. H.; Landry, C. C.; Stucky, G. K.; Chmelka, B. F.; Norby, P.; Hanson, J. C.; Monnier, A. *Chem. Mater.* **2001**, *13*, 2247.

templated silica materials. Choosing appropriate interaction parameters, it is possible to observe a two-phase region for the solvent/surfactant/inorganic ternary diagram. In this ternary diagram, a liquid crystal phase containing high surfactant and inorganic concentration is in equilibrium with a solvent-rich phase, and the structure of the liquid crystal phase depends on the temperature, surfactant architecture, and composition.

Independent of the solubility of the inorganic component in water, we observed the formation of hexagonal phases at low surfactant/inorganic ratios, while lamellar phases were favored at high surfactant/silica ratios. This is in agreement with experimental evidence,<sup>35</sup> and we indicate that modifying the interaction parameters could modify the type of structures observed at different overall compositions.

In the model we use, the surfactant solubility increases with temperature, and therefore, as temperature is increased, the concentration of surfactant in the liquid crystal phase decreases. This change in composition of the liquid crystal phase can produce a transformation between a lamellar and an hexagonal phase.

The principal limitations of our model are (a) the use of a cubic lattice, with a coordination number of 26, and (b) the primitive treatment of water, which neglects hydrogen bonding and other directional forces. In future work, we plan to relax these restrictions in an attempt to

obtain more quantitative agreement with experiment. The use of a cubic lattice overly restricts the possible bond lengths and angles, leading to quantitative disagreement with experiment. Such disagreement can be systematically reduced by the use of a discretized lattice, as suggested by Panagiotopoulos.<sup>38</sup> Even modest levels of discretization greatly increase the number of possible bond angles and lengths and greatly improve the results for phase equilibria. A more realistic treatment of water, using an orientation-dependent intermolecular potential, should improve the predicted temperature dependence of surfactant solubilities, phase boundaries, and micellar structures. Further improvement of the model should allow for the determination of the partition of different soluble silica species between the surfactant-rich phase and the solvent-rich phase.

**Acknowledgment.** We thank the Department of Energy for support of this research under Grant No. DE-FG02-98ER14847 and the National Partnership for Advanced Computational Infrastructure (Grant npa205) for providing supercomputer time at the San Diego Supercomputing Center.

LA026410D

---

(38) Panagiotopoulos, A. Z. *J. Chem. Phys.* **2000**, *112*, 7132.